

LOOPY: TAMING AUDIO-DRIVEN PORTRAIT AVATAR WITH LONG-TERM MOTION DEPENDENCY

Jianwen Jiang^{1*†}, Chao Liang^{1*}, Jiaqi Yang^{1*}, Gaojie Lin¹, Tianyun Zhong^{2‡}, Yanbo Zheng¹

¹ByteDance, ²Zhejiang University
 {jianwen.alan, liangchao.0412, yjq850207131}@gmail.com
 zhongtianyun@zju.edu.cn

<https://loopyavatar.github.io/>

ABSTRACT

With the introduction of diffusion-based video generation techniques, audio-conditioned human video generation has recently achieved significant breakthroughs in both the naturalness of motion and the synthesis of portrait details. Due to the limited control of audio signals in driving human motion, existing methods often add auxiliary spatial signals to stabilize movements, which may compromise the naturalness and freedom of motion. In this paper, we propose an end-to-end audio-only conditioned video diffusion model named Loopy. Specifically, we designed an inter- and intra-clip temporal module and an audio-to-latents module, enabling the model to leverage long-term motion information from the data to learn natural motion patterns and improving audio-portrait movement correlation. This method removes the need for manually specified spatial motion templates used in existing methods to constrain motion during inference. Extensive experiments show that Loopy outperforms recent audio-driven portrait diffusion models, delivering more lifelike and high-quality results across various scenarios.

1 INTRODUCTION

Due to the rapid advancements GAN and diffusion models in the field of video synthesis (Bar-Tal et al., 2024; Blattmann et al., 2023a;b; Guo et al., 2023; Zhou et al., 2022; Gupta et al., 2023; Wang et al., 2023; Ho et al., 2022; Brooks et al., 2022; Wang et al., 2020; Singer et al., 2022; Li et al., 2018; Villegas et al., 2022), human video synthesis (Siarohin et al., 2019; 2021; Xu et al., 2024b; Hu, 2024; Corona et al., 2024) has gradually approached the threshold of practical usability in terms of quality, attracting significant attention in recent years. Among these, zero-shot audio-driven portrait synthesis has seen an explosion of research (He et al., 2023; Tian et al., 2024; Xu et al., 2024a; Wang et al., 2024; Chen et al., 2024; Xu et al., 2024b; Stypulkowski et al., 2024) since around 2020, due to its ability to generate talking head videos with minimal barriers to entry. Starting last year, diffusion model techniques were introduced, with end-to-end audio-driven models (Tian et al., 2024; Xu et al., 2024a; Chen et al., 2024) demonstrating more vivid synthesis results compared to existing methods.

However, due to the weak correlation between audio and portrait motion, end-to-end audio-driven methods typically introduce additional conditions related to spatial motion to ensure temporal stability in the synthesized videos. Conditions such as face locators and speed layers (Tian et al., 2024; Xu et al., 2024a; Chen et al., 2024) restrict the range and velocity of portrait movements, potentially reducing the expressiveness of the final output, as illustrated in Figure 1. While the introduction of preset motion templates may mitigate this issue, it also introduces complications related to template selection, audio-motion synchronization, and repetitive template movements. From a model perspective, these limitations also hinder the full potential of video diffusion models in generating vivid motion. This paper aims to address this issue by proposing an audio-only conditioned portrait

*Equal Contribution

†Project Lead

‡Done during an internship at ByteDance.

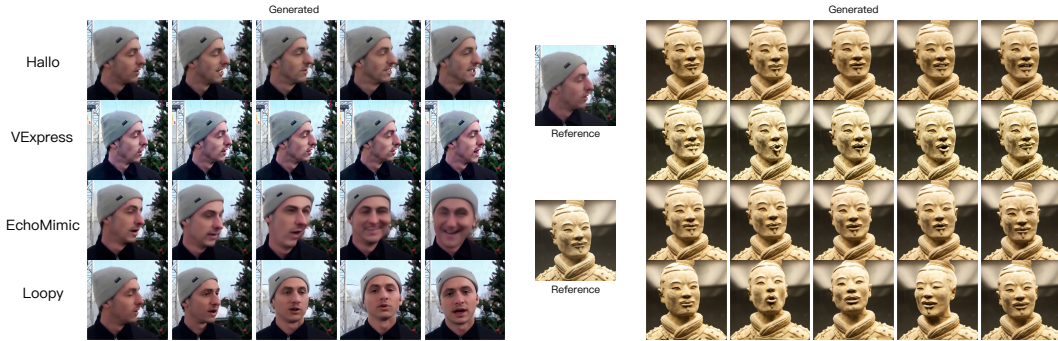


Figure 1: **Visual comparisons with existing methods.** Existing methods struggle to generate natural movements; compared to reference images, their motion, posture, and expressions often resemble the reference or remain nearly static due to the auxiliary spatial conditions. In contrast, Loopy effectively generates natural anthropomorphic movements solely from audio, including detailed head movements and facial expressions. Video results are provided in the supplementary materials.

diffusion model, enabling the model to learn natural motion patterns from data without the need for spatial templates.

We first attempted to remove structures such as the face locator and speed layer. This resulted in more frequent undesirable motion patterns in the synthesized videos, such as sudden temporal jitter, frame corruption, increased autoregressive degradation, and unnatural temporal details, leading to a decrease in overall quality. In practice, in current diffusion-based frameworks, the conditions influencing motion include not only audio (which maps to motion patterns in a many-to-many manner and is hard to fully define motions) but also motion frames. Motion frames provide appearance information from preceding clips, strongly influencing motion generation. However, current methods usually generate based on 4 motion frames from the last clip and over ten target frames from the current clip. At a typical 25 fps, this covers about 0.5 seconds in total, with motion frames covering only 0.2 seconds. Such short motion frames cause the model to primarily extract appearance information from the last clip rather than temporal motion information, such as motion style. For example, in the case of eye blinking, 0.2 seconds of preceding information is insufficient for the model to determine whether blinking should occur (it cannot know if blinking has occurred previously, making blinking a probabilistic event, which may lead to long periods without blinking in the generated video). When motion style is hard to determine by audio and motion frames, it exhibits randomness, necessitating additional guidance from spatial conditions such as face box and movement speed. We attempted to increase the length of motion frames and found that this approach can generate larger and more flexible movements to some extent, although it may lead to increased instability. This observation reminds us that increasing the temporal receptive field in an appropriate manner may help capture motion patterns more effectively and aid in generating natural motion. Additionally, current methods inject audio features into the diffusion model directly through cross-attention, which makes it difficult for the model to learn the relationship between audio and portrait motion, instead modeling the relationship between audio and all video pixels. This phenomenon is also mentioned in the Hallo (Xu et al., 2024a) work. The weak correlation between audio and portrait also increases the likelihood of generating random and unsatisfactory movements, making it difficult to generate natural motion that corresponds well with the audio.

Based on the above observations and considerations, we propose Loopy, an end-to-end template-free audio-conditioned diffusion model for portrait video generation, leveraging long-term motion dependency to generate vivid portrait videos. Specifically: for temporal aspect: We designed inter- and intra-clip temporal modules. Motion frames are modeled with a separate temporal layer to capture inter-clip temporal relationships, while the original temporal module focuses on intra-clip temporal modeling. Additionally, we introduced a temporal segment module to the intra-clip layer, extending the receptive field to over 100 frames (covering approximately 5 seconds at 25 fps, 30 times the original). For audio aspect: We introduced the audio-to-motion latents module, which transforms audio and facial motion-related features (landmarks, head motion variance, expression motion variance) into motion latents based on a shared feature space. These latents are inserted

into the denoising net as conditions. During testing, motion latents are generated using only audio. This approach allows weakly correlated audio to leverage strongly correlated motion conditions, enhancing the modeling of the relationship between audio and portrait motion. Extensive experiments validate that our design effectively improves the naturalness of motion and the robustness of video synthesis. In summary, our contributions include:

- (1) We propose a template-free audio-conditioned diffusion model for portrait video generation, featuring inter- and intra-clip temporal modules that leverage long-term motion dependency to learn natural motion patterns. Additionally, the audio-to-latents module enhances the correlation between audio and portrait motion by using strongly correlated conditions during training.
- (2) We validated the effectiveness of our method on public datasets and evaluated the model’s capabilities across various application scenarios (including multiple types of images and audio), demonstrating that our model achieves more vivid and stable synthesis results compared to existing methods.

2 RELATED WORKS

Audio-driven portrait video generation has attracted significant attention in recent years, with numerous works advancing the field. These methods can be categorized into GAN-based and diffusion-based approaches based on their video synthesis techniques.

GAN-based methods (Zhou et al., 2020; Prajwal et al., 2020; Zhang et al., 2023b; Liang et al., 2022) typically consist of two key components: an audio-to-motion model and a motion-to-video model. These models are usually implemented independently. For example, MakeItTalk (Zhou et al., 2020) uses an LSTM module to predict the landmark coordinates corresponding to the audio, and then a warp-based GAN model converts the landmark signals into video images. SadTalker (Zhang et al., 2023b) utilizes the existing FaceVid2Vid (Wang et al., 2021) method as the image synthesizer, employing ExpNet and PoseVAE to transform audio features into the inputs required by FaceVid2Vid, thereby completing the audio-to-video generation. With the introduction of diffusion techniques, some methods have implemented the audio-to-motion module using diffusion models while retaining the independent implementation of the motion-to-video module. For instance, GAIA (He et al., 2023) uses a VAE to represent motion as motion latents and implements a motion latents-to-video generation model. Additionally, it designs a diffusion model to achieve audio-to-motion latents generation, thereby enabling audio-to-video generation. DreamTalk (Ma et al., 2023), Dream-Talk (Zhang et al., 2023a), and VASA-1 (Xu et al., 2024b) propose similar ideas, using PIRender (Ren et al., 2021), FaceVid2Vid (Wang et al., 2021), and MegaPortrait (Drobyshev et al., 2022) as their motion-to-video models, respectively, and designing audio-to-motion representation models to complete the audio-to-portrait video generation process.

Apart from the above types, EMO Portrait (Tian et al., 2024) achieves audio-to-portrait video generation using a single diffusion model, replacing the two-stage independent design of the audio-to-motion module and the motion-to-video model. Hallo (Xu et al., 2024a), EchoMimic (Chen et al., 2024) and VExpress (Wang et al., 2024) have improved their audio-to-video modeling based on a similar audio-to-video diffusion framework. Although these end-to-end methods can generate vivid portrait videos, they need to introduce spatial condition module, like face locator and speed layer, to constrain head movements for stability, limiting the diversity of motion models in practical applications and hindering the full potential of diffusion models.

3 METHOD

In this section, we will introduce our method, Loopy. First, we will provide an overview of the framework, including the input, output, and key components of Loopy. Second, we will focus on the design of the inter-/intra-temporal modules, including the temporal segment module. Third, we will detail the implementation of the audio condition module. Finally, we will describe the implementation details during the training and testing of Loopy.

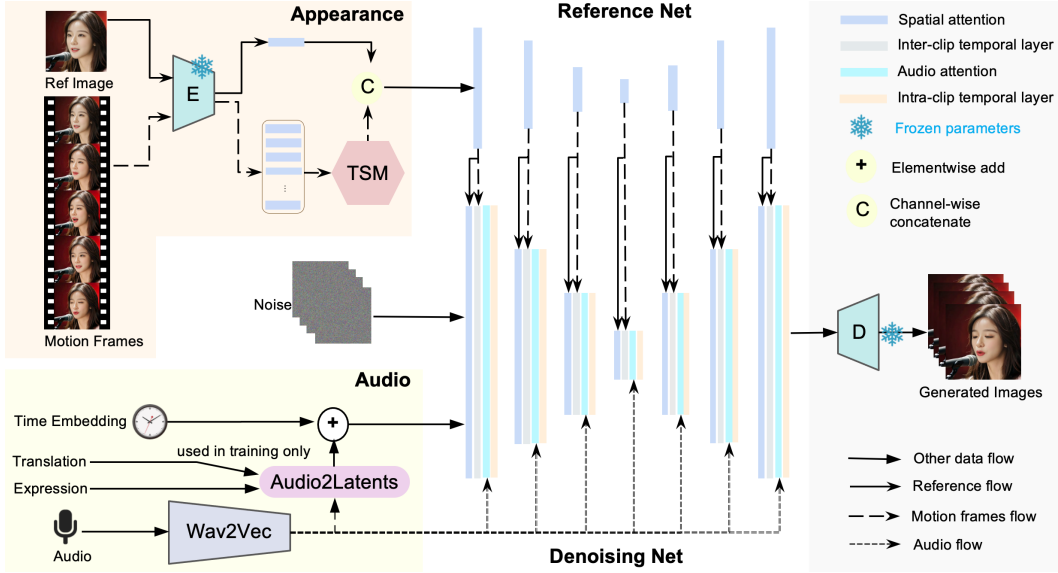


Figure 2: **The framework of Loopy.** it removes the commonly used face locator and speed layer modules found in existing methods. Instead, it achieves flexible and natural motion generation through the proposed inter/intra-clip temporal layer and audio-to-latents module.

3.1 FRAMEWORK

Our method is built upon Stable Diffusion (SD) and uses its initialization weights. SD is a text-to-image diffusion model based on the Latent Diffusion Model (LDM) (Rombach et al., 2022). It employs a pretrained VQ-VAE (Kingma, 2013; Van Den Oord et al., 2017) \mathcal{E} to transform images from pixel space to latent space. During training, images are first converted to latents, i.e., $z_0 = \mathcal{E}(I)$. Gaussian noise ϵ is then added to the latents in the latent space based on the Denoising Diffusion Probabilistic Model (DDPM) (Ho et al., 2020) for t steps, resulting in a noisy latent z_t . The denoising net takes z_t as input to predict ϵ . The training objective can be formulated as follows:

$$L = \mathbb{E}_{z_t, c, \epsilon \sim \mathcal{N}(0, 1), t} [\|\epsilon - \epsilon_\theta(z_t, t, c)\|_2^2], \quad (1)$$

where ϵ_θ represents the denoising net, including condition-related attention modules, which is the main part Loopy aims to improve. c represents the text condition embedding in SD, and in Loopy, it includes audio, motion frames, and other additional information influencing the final generation. During testing, the final image is obtained by sampling from Gaussian noise and removing the noise based on DDIM (Song et al., 2020) or DDPM.

As demonstrated in Figure 2, in the Loopy, the inputs to the denoising net include noisy latents, i.e., the VQ-VAE encoded image latents z_t . Unlike original SD, where the input is a single image, here it is a sequence of images representing a video clip. The inputs also include reference latents c_{ref} (encoded reference image latents via VQ-VAE), audio embedding c_{audio} (audio features of the current clip), motion frames c_{mf} (image latents of the M frames sequence from the preceding clips), and timestep t . During training, additional facial movement-related features are involved: c_{lmk} (facial keypoint sequence of the current clip), c_{mov} (head motion variance of the current clip), and c_{exp} (expression variance of the current clip). The output is the predicted noise ϵ . The denoising network employs a Dual U-Net architecture (Hu, 2024; Zhu et al., 2023). This architecture includes an additional reference net module, which replicates the original SD U-Net structure but utilizes reference latents c_{ref} as input. The reference net operates concurrently with the denoising U-Net. During the spatial attention layer computation in the denoising U-Net, the key and value features from corresponding positions in the reference net are concatenated with the denoising U-Net’s features along the token dimension before proceeding with the attention module computation. This design enables the denoising U-Net to effectively incorporate reference image features from the reference net.

Additionally, the reference net also takes motion frames latents c_{mf} as input for feature extraction, allowing these features to be utilized in subsequent temporal attention computations.

3.2 INTER/INTRA- CLIP TEMPORAL LAYERS DESIGN

Here, we introduce the design of the proposed inter-/intra-clip temporal modules. Unlike existing methods (Tian et al., 2024; Xu et al., 2024a; Chen et al., 2024; Wang et al., 2024) that process motion frame latents and noisy latents features simultaneously through a single temporal layer, Loopy employs two temporal attention layers: the inter-clip temporal layer and the intra-clip temporal layer. The inter-clip temporal layer first handles the cross-clip temporal relationships between motion frame latents and noisy latents, while the intra-clip temporal layer focuses on the temporal relationships within the noisy latents of the current clip.

First, we introduce the inter-clip temporal layer, initially ignoring the temporal segment module in Figure 2. We first collect the m image latents from the preceding clip, referred to as motion frames latents c_{mf} . Similar to c_{ref} , these latents are processed frame-by-frame through the reference network for feature extraction. Within each residual block, the features $x_{c_{mf}}$ obtained from the reference network are concatenated with the features x from the denoising U-Net along the temporal dimension. To distinguish the types of latents, we add learnable temporal embeddings. Subsequently, self-attention is computed on the concatenated tokens along the temporal dimension, referred to as temporal attention. The intra-clip temporal layer differs in that its input does not include features from motion frames latents, it only processes features from the noisy latents of the current clip. By separating the dual temporal layers, the model can better handle the aggregation of different semantic temporal features in cross-clip temporal relationships.

Due to the independent design of the inter-clip temporal layer, Loopy is better equipped to model the motion relationships among clips. To enhance this capability, we introduce the temporal segment module before c_{mf} enters the reference network. This module not only extends the temporal range covered by the inter-clip temporal layer but also accounts for the variations in information due to the varying distances of different clips from the current clip, as illustrated in Figure 3. The temporal segment module divides the original motion frame into multiple segments and extracts representative motion frames from each segment to abstract the segment. Based on these abstracted motion frames, we recombine them to

obtain motion frame latents for subsequent computations. For the segmentation process, we define two hyperparameters: stride s and expand ratio r . The stride s represents the number of abstract motion frames in each segment, while the expand ratio r is used to calculate the length of the original motion frames in each segment. The number of frames in the i -th segment, ordered from closest to farthest from the current clip, is given by $s \times r^{(i-1)}$. For example, with a stride $s = 4$ and an expand ratio $r = 2$, the first segment would contain 4 frames, the second segment would contain 8 frames, and the third segment would contain 16 frames. For the abstraction process after segmentation, we default to uniform sampling within each segment. In the experimental section, we investigate different segmentation parameters and abstraction methods. Since segmentation and abstraction directly affect the learning of long-term motion dependency, different methods have a significant impact on the results. The output of the temporal segment module, c_{mf}^o , can be defined as:

$$c_{mf,i}^o = c_{mf, \lfloor \frac{\text{start_index}_i + \text{end_index}_i}{2} \rfloor} \tag{2}$$

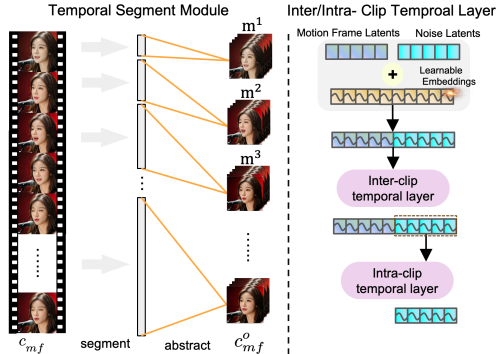


Figure 3: **The illustration of the temporal segment module and the inter/intra-clip temporal layers.** The former allows us to expand the motion frame to cover over 100 frames, while the later enables the modeling of long-term motion dependency.

where $\text{start_index}_i = \sum_{j=0}^{k-1} r^j \cdot s$ and $\text{end_index}_i = \text{start_index}_i + r^k \cdot s$, with $k = \lfloor \frac{i}{s} \rfloor$. $c_{mf,i}^o$ represents the mean value of the i -th element of the output, calculated from the sequence c_{mf} .

The temporal segment module rapidly expands the temporal coverage of the motion frames input to the inter-clip temporal layer while maintaining acceptable computational complexity. For closer frames, a lower expansion rate retains more details, while for distant frames, a higher expansion rate covers a longer duration. This approach helps the model better capture motion style from long-term information and generate temporally natural motion without spatial templates.

3.3 AUDIO CONDITION MODULE

For the audio condition, we first use wav2vec (Baevski et al., 2020; Schneider et al., 2019) for audio feature extraction. Following the approach in EMO, we concatenate the hidden states from each layer of the wav2vec network to obtain multi-scale audio features. For each video frame, we concatenate the audio features of the two preceding and two succeeding frames, resulting in a 5-frame audio feature as audio embeddings c_{audio} for the current frame. Initially, in each residual block, we use cross-attention with noisy latents as the query and audio embedding c_{audio} as the key and value to compute an attended audio feature. This attended audio feature is then added to the noisy latents feature obtained from self-attention, resulting in a new noisy latents feature. This provides a preliminary audio condition.

Additionally, as illustrated in Figure 4, we introduce the Audio-to-Latents module. This module maps conditions that have both strong and weak correlations with portrait motion, such as audio, to a shared motion latents space. These mapped conditions serve as the final condition features, thereby enhancing the modeling of the relationship between audio and portrait movements based on motion latents. Specifically, we maintain a set of learnable embeddings. For each input condition, we map it to a query feature using a fully connected (FC) layer, while the learnable embeddings serve as key and value features for attention computation to obtain a new feature based on the learnable embeddings. These new features, referred to as motion latents, replace the input condition in subsequent computations. These motion latents are then dimensionally transformed via an FC layer and added to the timestep embedding features for subsequent network computation. During training, we sample an input condition for the Audio-to-Latents module with equal probability from audio embeddings and facial movement-related features such as landmarks, face absolute motion variance, and face expression motion variance. During testing, we only input audio to generate motion latents. By leveraging features strongly correlated with portrait movement, the model utilizes learnable embeddings to control motion. Consequently, transforming audio embeddings into motion latents can also allow for more direct influence on portrait motion.

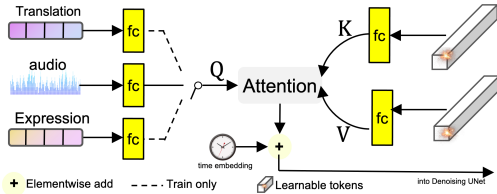


Figure 4: **The audio-to-latents module.**

3.4 TRAINING STRATEGIES

Conditions Mask and Dropout. In the Loopy framework, various conditions are involved, including the reference image c_{ref} , audio features c_{audio} , preceding frame motion frames c_{mf} , and motion latents c_{ml} representing audio and facial motion conditions. Due to the overlapping nature of the information contained within these conditions, to better learn the unique information specific to each condition, we used distinct masking strategies for the conditions during the training process. During training, c_{audio} and motion latents are masked to all-zero features with a 10% probability. For c_{ref} and c_{mf} , we design specific dropout and mask strategies due to their conflicting relationship. c_{mf} also provides appearance information and is closer to the current clip compared to c_{ref} , leading the model to heavily rely on motion frames rather than the reference image. This can cause color shifts and artifacts in long video sequences during inference. To address this, c_{ref} has a 15% probability of being dropped, meaning the denoising U-Net will not concatenate features from the reference network during self-attention computation. When c_{ref} is dropped, motion frames are also dropped, meaning the denoising U-Net will not concatenate features from the reference network during temporal

attention computation. Additionally, motion frames have an independent 40% probability of being masked to all-zero features.

Multistage Training. Following AnimateAnyone (Hu, 2024) and EMO (Tian et al., 2024), we employ a 2-stage training process. In the first stage, the model is trained without temporal layers and the audio condition module. The inputs to the model are the noisy latents of the target single-frame image and reference image latents, focusing the model on an image-level pose variations task. After completing the first stage, we proceed to the second stage, where the model is initialized with the reference network and denoising U-Net from the first stage. We then add the inter-/intra-clip temporal layers and the audio condition module for full training to obtain the final model.

Inference. During Inference, we perform class-free guidance (Ho & Salimans, 2022) using multiple conditions. Specifically, we conduct three inference runs, differing in whether certain conditions are dropped. The final noise e_{final} is computed as:

$$e_{final} = \text{audio_ratio} \times (e_{audio} - e_{ref}) + \text{ref_ratio} \times (e_{ref} - e_{base}) + e_{base}$$

where e_{audio} includes all conditions $c_{ref}, c_{audio}, c_{mf}, c_{ml}, e_{ref}$ but mask c_{audio} to all-zero features, and e_{base} masks c_{audio} to all-zero features and removes the concatenation of reference network features in the denoising U-Net’s self-attention. This approach allows us to control the model’s final output in terms of adherence to the reference image and alignment with the audio. The audio ratio is set to 5 and the reference ratio is set to 3. We use DDIM sampling with 25 denoising steps to complete the inference.

3.5 EXPERIMENTS

Datasets. For training Data, We collected talking head video data from the internet, excluding videos with low lip sync scores, excessive head movement, extreme rotation, or incomplete head exposure. This resulted in 160 hours of cleaned training data. Additionally, we supplemented the training data with public datasets such as HDTF (Zhang et al., 2021). For the test set, we randomly sampled 100 videos from CelebV-HQ (Zhu et al., 2022) (a public high-quality celebrity video dataset with mixed scenes) and RAVDESS (Kaggle) (a public high-definition indoor talking scene dataset with rich emotions). To test the generalization ability of diffusion-based models, we also collected 20 portrait test images, including real people, anime, side face, and humanoid crafts of different materials, along with 20 audio clips, including speeches, singing, rap and emotionally rich speech. We refer to this test set as the openset test set.

Implementation Details. We trained our model using 24 Nvidia A100 GPUs with a batch size of 24, using the AdamW (Loshchilov & Hutter, 2017) optimizer with a learning rate of $1e-5$. The generated video length was set to 12 frames, and the motion frame length was set to 124 frames, representing the preceding 124 frames of the current 12-frame video. After temporal squeezing, this was compressed to 20 motion frame latents. During training, the reference image was randomly selected from a frame within the video clip. For the facial motion information required to train audio-to-motion module, we used DWPose (Yang et al., 2023) to detect facial keypoints for the current 12 frames. The variance of the absolute position of the nose tip across these 12 frames was used as the absolute head motion variance. The variance of the displacement of the upper half of the facial keypoints (37 keypoints) relative to the nose tip across these 12 frames was used as the expression variance. The training videos were uniformly processed at 25 fps and cropped to 512x512 portrait videos.

Metrics. We assess image quality with the IQA metric (Wu et al., 2023), video motion with VBench’s smooth metric (Huang et al., 2024), and audio-visual synchronization using SyncC and SyncD (Prajwal et al., 2020). For the CelebVHQ and RAVDESS test sets, which have corresponding ground truth videos, we will also compute FVD (Unterthiner et al., 2019), E-FID (Tian et al., 2024) and FID metrics for comparison. Additionally, to compare the global motion (denoted as Glo) and dynamic expressions (denoted as Exp) of the portrait, we calculated the variance values based on key points of the nose and the upper face, specifically excluding the mouth area. We also computed the values for the ground truth video as a reference for comparison. For the openset testset, which lacks ground truth video references, we conducted subjective evaluations. Ten experienced users were invited to assess six key dimensions: identity consistency, video synthesis quality, audio-emotion

Table 1: Comparisons with existing methods on the CelebV-HQ test set.

Method	IQA \uparrow	Sync-C \uparrow	Sync-D \downarrow	FVD-Res \downarrow	FVD-Inc \downarrow	FID \downarrow	Smooth \uparrow	Glo	Exp	E-FID \downarrow
SadTalker	2.953	3.843	8.765	171.848	1746.038	36.648	0.9964	0.554	0.270	2.248
Hallo	3.505	4.130	9.079	53.992	742.974	35.961	0.9946	0.499	0.255	2.426
VExpress	2.946	3.547	9.415	117.868	1356.510	65.098	0.9957	0.020	0.166	2.414
EchoMimic	3.307	3.136	10.378	54.715	828.966	35.373	0.9926	2.259	0.640	3.018
GT	-	-	-	-	-	-	0.9937	3.249	0.506	-
Loopy	3.780	4.849	8.196	49.153	680.634	33.204	0.9949	2.233	0.452	<u>2.307</u>

Table 2: Comparisons with existing methods on the RAVDESS test set.

Method	IQA \uparrow	Sync-C \uparrow	Sync-D \downarrow	FVD-Res \downarrow	FVD-Inc \downarrow	FID \downarrow	Smooth \uparrow	Glo	Exp	E-FID \downarrow
SadTalker	3.840	4.304	7.621	22.516	487.924	32.343	0.9955	0.604	0.120	3.270
Hallo	4.393	4.062	8.552	38.471	537.478	19.826	0.9942	0.194	0.080	3.785
VExpress	3.690	5.001	7.710	62.388	982.810	26.736	0.9962	0.007	0.039	3.901
EchoMimic	4.504	3.292	9.096	54.115	688.675	21.058	0.9924	0.641	0.184	3.350
GT	-	-	-	-	-	-	0.9917	3.335	0.317	-
Loopy	4.506	<u>4.814</u>	<u>7.798</u>	16.134	394.288	17.017	0.9923	2.962	0.343	3.132

matching, motion diversity, naturalness of motion, and lip-sync accuracy. For each case, participants were required to identify the top-performing method in each dimension.

3.5.1 RESULTS AND ANALYSIS

Performance in Complex Scenarios. CelebV-HQ includes videos of celebrities speaking in various scenarios, including films and interviews, both indoors and outdoors, with diverse portrait poses. This makes testing on this dataset effectively simulate real-world usage conditions. As shown in Table 1, our method significantly outperforms the compared methods in most metrics, as evidenced by the comparison videos provided in the supplementary materials. Regarding motion-related metrics, although not the best, our results are similar to those of the ground truth in terms of smoothness. In the dynamic expression metric (Exp), our method closely matches GT, more so than the compared methods. For global motion (Glo), our performance is similar to that of EchoMimic. However, it is evident that our method has a distinct advantage in video synthesis quality and lip-sync accuracy.

Performance in Emotional Expression. RAVDESS is a high-definition talking scene dataset containing videos with varying emotional intensities. It effectively evaluates the method’s performance in emotional expression. As demonstrated by the E-FID (Tian et al., 2024) metric, our method outperforms the compared methods. This is corroborated in the motion dynamics metrics Glo and Exp, where our results are closer to the ground truth. Although our lip-sync accuracy is slightly inferior to VExpress, it is important to note that the results generated by VExpress generally lack dynamic motion, as indicated by the Glo, Exp, and E-FID metrics. This static nature can provide an advantage when measured with SyncNet for lip-sync accuracy.

Performance in Openset Scenarios. We compared different input styles (real people, anime, humanoid crafts and sife face) and various types of audio (speech, singing, rap, and emotional audio) to evaluate the robustness of the methods. As shown in Table 3, Loopy consistently outperforms the compared methods across these diverse scenarios.

3.5.2 ABLATION STUDIES

Analysis of Key Components. We analyzed the impact of the two key components of the Loopy, the inter/intra-clip temporal layer and the audio-to-latents module. For the former, we conducted two experiments: (1) removing the dual temporal layer design and retaining a single temporal layer to handle the temporal relationships of both the last and current clips, similar to methods like EMO and Hallo; (2) removing the temporal segment module and retaining the design of 4 motion frames as in other methods. For the latter, we removed the audio-to-latents module and retained only cross-attention for audio feature injection. The results, listed in Table 3, show that the dual temporal

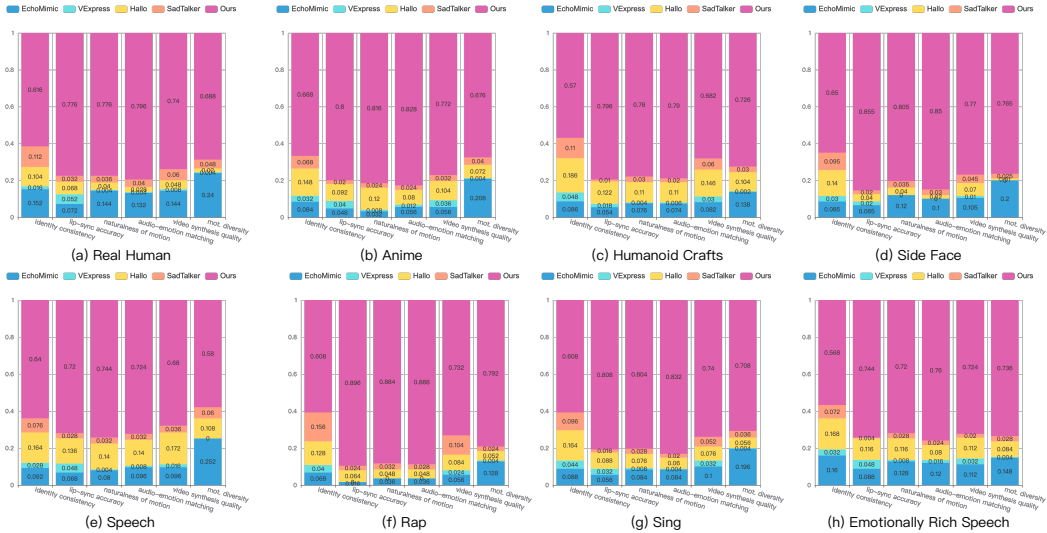


Figure 5: User voting comparisons on the openset test set. The first row includes experimental results for various categories of input images, while the second row includes experimental results for various categories of input audio.

Table 3: Experiments on the effectiveness of the proposed modules.

Method	IQA \uparrow	Sync-C \uparrow	Sync-D \downarrow	smooth \uparrow
Full Model	4.507	6.303	7.749	0.9932
w/o inter-clip temp.	4.335	6.104	8.129	0.9942
w/o TSM	4.386	6.054	8.235	0.9922
w/o A2L	4.428	5.999	8.351	0.9922
single temp. + 20 mf	4.072	6.201	8.309	0.9752
$s = 1, r = 2$	4.461	5.919	8.245	0.9940
$s = 2, r = 2$	4.453	5.855	8.326	0.9930
$s = 3, r = 2$	4.443	6.083	8.161	0.9930
$s = 4, r = 1$	4.424	6.219	8.004	0.9931
mean sample	4.452	5.907	8.199	0.9931
random sample	4.438	6.098	8.144	0.9932

layer design improves temporal stability and image quality, and its removal leads to performance degradation. Removing the temporal segment module prevents the model from learning motion style information from long-term motion dependency, resulting in a decline in overall motion quality, including expressiveness and temporal stability. Removing the audio-to-latents module also reduces the overall quality of synthesized visuals and motion. This is because, during the training of the audio-to-latents module, spatial conditions are added for mixed training. Spatial conditions provide clearer motion guidance compared to audio alone, facilitating easier model convergence. These results validate the effectiveness of our method.

Impact of Long-Term Temporal Dependency. We also investigated the impact of long-term motion dependency on the results and list the results in Table 3. Initially, we compared the effects of extending the motion frame length to 20 under a single temporal layer setting. We observed that while this approach enhances the dynamics of the model’s output, it significantly degrades the overall image quality. In contrast, on the full model with 20 motion frames ($s = 4, r = 1$), the addition of inter/intra-clip temporal layers indeed improved the overall results. Regarding the settings of s and r , we experimented with various values. Starting with a fixed $r = 2$, we found that smaller values of s resulted in poorer overall performance. We attribute this to the disparity in FPS between the target and motion frames, which complicates inter-clip temporal modeling due to the lower proportion of motion frames. As s increases, the number of motion frames also increases, allowing the inter-clip temporal layer to effectively model cross-clip temporal relationships, thereby significantly enhancing

overall performance. We also compared the effects of r with the same $s = 4$, where $r = 1$. A smaller r indicates a narrower temporal coverage, which slightly reduces performance compared to the full model ($s = 4, r = 2$). Finally, we explored different sampling strategies for motion frames within the temporal segment module, comparing methods such as average pooling and random single-frame sampling. The uniform sampling approach of the full model proved more effective, likely because it provides more stable interval information, which benefits the inter-clip temporal layer in learning long-term motion information.



Figure 6: Visualization of videos generated by Loopy in different scenarios.

3.5.3 VISUAL RESULTS ANALYSIS

We provide visual analysis for the openset scenarios in Figure 6. Compared to other methods, Loopy demonstrates significant advantages in ID preservation, motion amplitude, and image quality. It also performs well with uncommon images. Additional video results are available in the supplementary materials.

4 CONCLUSION

In this paper, we propose LOOPY, an end-to-end audio-driven portrait video generation framework that does not require spatial conditions and leverages long-term motion dependency to learn natural motion patterns from data. Specifically, we introduce the inter/intra-clip temporal layer design and the audio-to-latents module, which enhance the model’s ability to learn the correlation between audio and portrait motion from temporal and audio dimensions, respectively. Extensive experiments validate the

effectiveness of our method, demonstrating significant improvements in temporal stability, motion diversity, and overall video quality over existing methods.

REFERENCES

- Alexei Baevski, Yuhao Zhou, Abdelrahman Mohamed, and Michael Auli. wav2vec 2.0: A framework for self-supervised learning of speech representations. Advances in neural information processing systems, 33:12449–12460, 2020.
- Omer Bar-Tal, Hila Chefer, Omer Tov, Charles Herrmann, Roni Paiss, Shiran Zada, Ariel Ephrat, Junhua Hur, Yuanzhen Li, Tomer Michaeli, et al. Lumiere: A space-time diffusion model for video generation. arXiv preprint arXiv:2401.12945, 2024.
- Andreas Blattmann, Tim Dockhorn, Sumith Kulal, Daniel Mendelevitch, Maciej Kilian, Dominik Lorenz, Yam Levi, Zion English, Vikram Voleti, Adam Letts, et al. Stable video diffusion: Scaling latent video diffusion models to large datasets. arXiv preprint arXiv:2311.15127, 2023a.
- Andreas Blattmann, Robin Rombach, Huan Ling, Tim Dockhorn, Seung Wook Kim, Sanja Fidler, and Karsten Kreis. Align your latents: High-resolution video synthesis with latent diffusion models. In Proceedings of the IEEE/CVF Conference on Computer Vision and Pattern Recognition, pp. 22563–22575, 2023b.
- Tim Brooks, Janne Hellsten, Miika Aittala, Ting-Chun Wang, Timo Aila, Jaakko Lehtinen, Ming-Yu Liu, Alexei Efros, and Tero Karras. Generating long videos of dynamic scenes. Advances in Neural Information Processing Systems, 35:31769–31781, 2022.
- Zhiyuan Chen, Jiajiong Cao, Zhiquan Chen, Yuming Li, and Chenguang Ma. Echomimic: Life-like audio-driven portrait animations through editable landmark conditions. arXiv preprint arXiv:2407.08136, 2024.
- Enric Corona, Andrei Zanfir, Eduard Gabriel Bazavan, Nikos Kolotouros, Thiemo Alldieck, and Cristian Sminchisescu. Vlogger: Multimodal diffusion for embodied avatar synthesis. arXiv preprint arXiv:2403.08764, 2024.
- Nikita Drobyshev, Jenya Chelishev, Taras Khakhulin, Aleksei Ivakhnenko, Victor Lempitsky, and Egor Zakharov. Megaportraits: One-shot megapixel neural head avatars. In Proceedings of the 30th ACM International Conference on Multimedia, pp. 2663–2671, 2022.
- Yuwei Guo, Ceyuan Yang, Anyi Rao, Zhengyang Liang, Yaohui Wang, Yu Qiao, Maneesh Agrawala, Dahua Lin, and Bo Dai. Animatediff: Animate your personalized text-to-image diffusion models without specific tuning. arXiv preprint arXiv:2307.04725, 2023.
- Agrim Gupta, Lijun Yu, Kihyuk Sohn, Xiuye Gu, Meera Hahn, Li Fei-Fei, Irfan Essa, Lu Jiang, and José Lezama. Photorealistic video generation with diffusion models. arXiv preprint arXiv:2312.06662, 2023.
- Tianyu He, Junliang Guo, Runyi Yu, Yuchi Wang, Jialiang Zhu, Kaikai An, Leyi Li, Xu Tan, Chunyu Wang, Han Hu, et al. Gaia: Zero-shot talking avatar generation. arXiv preprint arXiv:2311.15230, 2023.
- Jonathan Ho and Tim Salimans. Classifier-free diffusion guidance. arXiv preprint arXiv:2207.12598, 2022.
- Jonathan Ho, Ajay Jain, and Pieter Abbeel. Denoising diffusion probabilistic models. Advances in neural information processing systems, 33:6840–6851, 2020.
- Jonathan Ho, Tim Salimans, Alexey Gritsenko, William Chan, Mohammad Norouzi, and David J Fleet. Video diffusion models. Advances in Neural Information Processing Systems, 35:8633–8646, 2022.
- Li Hu. Animate anyone: Consistent and controllable image-to-video synthesis for character animation. In Proceedings of the IEEE/CVF Conference on Computer Vision and Pattern Recognition, pp. 8153–8163, 2024.

- Ziqi Huang, Yinan He, Jiashuo Yu, Fan Zhang, Chenyang Si, Yuming Jiang, Yuanhan Zhang, Tianxing Wu, Qingyang Jin, Nattapol Chanpaisit, et al. Vbench: Comprehensive benchmark suite for video generative models. In Proceedings of the IEEE/CVF Conference on Computer Vision and Pattern Recognition, pp. 21807–21818, 2024.
- Kaggle. Ravdess emotional speech audio. <https://www.kaggle.com/datasets/uwrfkagglers/ravdess-emotional-speech-audio>.
- DP Kingma. Auto-encoding variational bayes. arXiv preprint arXiv:1312.6114, 2013.
- Yitong Li, Martin Min, Dinghan Shen, David Carlson, and Lawrence Carin. Video generation from text. In Proceedings of the AAAI conference on artificial intelligence, volume 32, 2018.
- Borong Liang, Yan Pan, Zhizhi Guo, Hang Zhou, Zhibin Hong, Xiaoguang Han, Junyu Han, Jingtuo Liu, Errui Ding, and Jingdong Wang. Expressive talking head generation with granular audio-visual control. In Proceedings of the IEEE/CVF Conference on Computer Vision and Pattern Recognition (CVPR), pp. 3387–3396, June 2022.
- Ilya Loshchilov and Frank Hutter. Decoupled weight decay regularization. arXiv preprint arXiv:1711.05101, 2017.
- Yifeng Ma, Shiwei Zhang, Jiayu Wang, Xiang Wang, Yingya Zhang, and Zhidong Deng. Dreamtalk: When expressive talking head generation meets diffusion probabilistic models. arXiv preprint arXiv:2312.09767, 2023.
- KR Prajwal, Rudrabha Mukhopadhyay, Vinay P Nambodiri, and CV Jawahar. A lip sync expert is all you need for speech to lip generation in the wild. In Proceedings of the 28th ACM international conference on multimedia, pp. 484–492, 2020.
- Yurui Ren, Ge Li, Yuanqi Chen, Thomas H Li, and Shan Liu. Pirenderer: Controllable portrait image generation via semantic neural rendering. In Proceedings of the IEEE/CVF international conference on computer vision, pp. 13759–13768, 2021.
- Robin Rombach, Andreas Blattmann, Dominik Lorenz, Patrick Esser, and Björn Ommer. High-resolution image synthesis with latent diffusion models. In Proceedings of the IEEE/CVF conference on computer vision and pattern recognition, pp. 10684–10695, 2022.
- Steffen Schneider, Alexei Baevski, Ronan Collobert, and Michael Auli. wav2vec: Unsupervised pre-training for speech recognition. arXiv preprint arXiv:1904.05862, 2019.
- Aliaksandr Siarohin, Stéphane Lathuilière, Sergey Tulyakov, Elisa Ricci, and Nicu Sebe. First order motion model for image animation. Advances in neural information processing systems, 32, 2019.
- Aliaksandr Siarohin, Oliver J Woodford, Jian Ren, Menglei Chai, and Sergey Tulyakov. Motion representations for articulated animation. In Proceedings of the IEEE/CVF Conference on Computer Vision and Pattern Recognition, pp. 13653–13662, 2021.
- Uriel Singer, Adam Polyak, Thomas Hayes, Xi Yin, Jie An, Songyang Zhang, Qiyuan Hu, Harry Yang, Oron Ashual, Oran Gafni, et al. Make-a-video: Text-to-video generation without text-video data. arXiv preprint arXiv:2209.14792, 2022.
- Jiaming Song, Chenlin Meng, and Stefano Ermon. Denoising diffusion implicit models. arXiv preprint arXiv:2010.02502, 2020.
- Michal Stypulkowski, Konstantinos Vougioukas, Sen He, Maciej Zieba, Stavros Petridis, and Maja Pantic. Diffused heads: Diffusion models beat gans on talking-face generation. In Proceedings of the IEEE/CVF Winter Conference on Applications of Computer Vision, pp. 5091–5100, 2024.
- Linrui Tian, Qi Wang, Bang Zhang, and Liefeng Bo. Emo: Emote portrait alive-generating expressive portrait videos with audio2video diffusion model under weak conditions. arXiv preprint arXiv:2402.17485, 2024.
- Thomas Unterthiner, Sjoerd van Steenkiste, Karol Kurach, Raphaël Marinier, Marcin Michalski, and Sylvain Gelly. Fvd: A new metric for video generation. 2019.

- Aaron Van Den Oord, Oriol Vinyals, et al. Neural discrete representation learning. Advances in neural information processing systems, 30, 2017.
- Ruben Villegas, Mohammad Babaeizadeh, Pieter-Jan Kindermans, Hernan Moraldo, Han Zhang, Mohammad Taghi Saffar, Santiago Castro, Julius Kunze, and Dumitru Erhan. Phenaki: Variable length video generation from open domain textual descriptions. In International Conference on Learning Representations, 2022.
- Cong Wang, Kuan Tian, Jun Zhang, Yonghang Guan, Feng Luo, Fei Shen, Zhiwei Jiang, Qing Gu, Xiao Han, and Wei Yang. V-express: Conditional dropout for progressive training of portrait video generation. arXiv preprint arXiv:2406.02511, 2024.
- Jiuniu Wang, Hangjie Yuan, Dayou Chen, Yingya Zhang, Xiang Wang, and Shiwei Zhang. Mod-elscope text-to-video technical report. arXiv preprint arXiv:2308.06571, 2023.
- Ting-Chun Wang, Arun Mallya, and Ming-Yu Liu. One-shot free-view neural talking-head synthesis for video conferencing. In Proceedings of the IEEE Conference on Computer Vision and Pattern Recognition, 2021.
- Yaohui Wang, Piotr Bilinski, Francois Bremond, and Antitza Dantcheva. Imaginator: Conditional spatio-temporal gan for video generation. In Proceedings of the IEEE/CVF Winter Conference on Applications of Computer Vision, pp. 1160–1169, 2020.
- Haoning Wu, Zicheng Zhang, Weixia Zhang, Chaofeng Chen, Liang Liao, Chunyi Li, Yixuan Gao, Annan Wang, Erli Zhang, Wenxiu Sun, et al. Q-align: Teaching Imms for visual scoring via discrete text-defined levels. arXiv preprint arXiv:2312.17090, 2023.
- Mingwang Xu, Hui Li, Qingkun Su, Hanlin Shang, Liwei Zhang, Ce Liu, Jingdong Wang, Luc Van Gool, Yao Yao, and Siyu Zhu. Hallo: Hierarchical audio-driven visual synthesis for portrait image animation. arXiv preprint arXiv:2406.08801, 2024a.
- Sicheng Xu, Guojun Chen, Yu-Xiao Guo, Jiaolong Yang, Chong Li, Zhenyu Zang, Yizhong Zhang, Xin Tong, and Baining Guo. Vasa-1: Lifelike audio-driven talking faces generated in real time. arXiv preprint arXiv:2404.10667, 2024b.
- Zhendong Yang, Ailing Zeng, Chun Yuan, and Yu Li. Effective whole-body pose estimation with two-stages distillation. In Proceedings of the IEEE/CVF International Conference on Computer Vision, pp. 4210–4220, 2023.
- Chenxu Zhang, Chao Wang, Jianfeng Zhang, Hongyi Xu, Guoxian Song, You Xie, Linjie Luo, Yapeng Tian, Xiaohu Guo, and Jiashi Feng. Dream-talk: diffusion-based realistic emotional audio-driven method for single image talking face generation. arXiv preprint arXiv:2312.13578, 2023a.
- Wenxuan Zhang, Xiaodong Cun, Xuan Wang, Yong Zhang, Xi Shen, Yu Guo, Ying Shan, and Fei Wang. Sadtalker: Learning realistic 3d motion coefficients for stylized audio-driven single image talking face animation. In Proceedings of the IEEE/CVF Conference on Computer Vision and Pattern Recognition, pp. 8652–8661, 2023b.
- Zhimeng Zhang, Lincheng Li, Yu Ding, and Changjie Fan. Flow-guided one-shot talking face generation with a high-resolution audio-visual dataset. In Proceedings of the IEEE/CVF Conference on Computer Vision and Pattern Recognition, pp. 3661–3670, 2021.
- Daquan Zhou, Weimin Wang, Hanshu Yan, Weiwei Lv, Yizhe Zhu, and Jiashi Feng. Magicvideo: Efficient video generation with latent diffusion models. arXiv preprint arXiv:2211.11018, 2022.
- Yang Zhou, Xintong Han, Eli Shechtman, Jose Echevarria, Evangelos Kalogerakis, and Dingzeyu Li. Makelttalk: speaker-aware talking-head animation. ACM Transactions On Graphics (TOG), 39(6):1–15, 2020.
- Hao Zhu, Wayne Wu, Wentao Zhu, Liming Jiang, Siwei Tang, Li Zhang, Ziwei Liu, and Chen Change Loy. Celebv-hq: A large-scale video facial attributes dataset. In European conference on computer vision, pp. 650–667. Springer, 2022.

Luyang Zhu, Dawei Yang, Tyler Zhu, Fitsum Reda, William Chan, Chitwan Saharia, Mohammad Norouzi, and Ira Kemelmacher-Shlizerman. Tryondiffusion: A tale of two unets. In Proceedings of the IEEE/CVF Conference on Computer Vision and Pattern Recognition, pp. 4606–4615, 2023.